

Content Based Image Retrieval system using Feature Coding

Yogesh Bhila Patil¹, Prof. Kailash Patidar²

PG Scholar, Dept. Of Computer Science & Engg., SSSIST, Sehore, M.P., India¹

HOD, Dept. Of Computer Science & Engg., SSSIST, Sehore, M.P., India²

ABSTRACT—Image retrieval used in CBIR is based on image features viz. color, texture, shape, size etc. CBIR system is used in various areas like medical, academic, art, fashion, entertainment. Image classification framework projects a linear training complexity and great interpretability which is missing in customary models. Feature coding which is a key component of image classification, greatly influences in terms of both accuracy and speed. For this, the most imminent BoF framework is used. There are numbers of feature coding techniques available. Out of these techniques, Super Vector Coding (SVC) outperforms in both speed and accuracy, as it reconstructs a feature without deviation.

KEYWORDS - Super Vector Coding (SVC), Feature coding, CBIR, bag-of-features (BoF), image classification.

I. INTRODUCTION

The most promising computer technique i.e. content based image retrieval is used to solve searching problem for digital image in the huge database. In content based image retrieval, various image features such as color, texture and shape are considered for retrieving an image. For getting these features, Feature Extraction technique is projected. To increase speed of retrieving an image in enormous databases and to increase accuracy of retrieval, Image classification or categorization is proposed. Image classification is a machine learning approach. For image classification, in conventional statistical approaches only gray values are used. For enhanced and effective retrieval results, various innovative techniques such as Genetic Algorithms (GA), Support Vector Machines (SVM), Fuzzy measures, Artificial Neural Networks (ANN), and Genetic Algorithms through Neural Networks can be used.

II. LITERATURE REVIEW

In paper [2], Accurate Legendre Moments (ALM) based content based image retrieval system is proposed for gray scale images. In this system, they worked on shape feature of image, for image classification. As SVM is a kernel method and kernel function in SVM plays important role in determining performance, with appropriate parameters a kernel function should be preferred. The choice of kernel and tuning of appropriate parameters is the most challenging problem. The image classification efficiency is improved by retaining Support Vector Machine (SVM) classifier.

For content based image classification [4], a nonparametric approach is proposed. In this paper, classification system is proposed which allows distinguishing and improving the cluster of a query image based on its content. CBIR system designates each image by automatically extracted set of features. Then, the obtained feature vectors are specified as an input to a classifier. The various descriptors and practices are used for the practices of image feature selection and extraction such as Bag-of-Words (BoW), scale invariant feature transform (SIFT), and spatial histograms (SP). The naive bayes nearest neighbor (NBNN) algorithm, which belongs to the category of non-parametric classifiers, is used for the classifier. In image classification, other classifiers are also used, that are described briefly.

In paper [3], SVM used as a classifier for classification of various image categories and obtained optimal result. Accuracy and error rate should be found to obtain precise result. This method contributes much enhanced performance than the traditional method of image retrieval. With the help of classification technology, image similarity accomplished by conjoining multiple feature distances [26]. A new twostep strategy developed to handle the noisy positive examples, which integrating the methods of data cleaning and noisetolerant classifier. To validate the effectiveness of the CBIR using SVM algorithm, the extensive experiments carried out on two different real image collections.

III. IMPLEMENTATION DETAILS

To link feature extraction and feature pooling [24, 25], core component of image classification is used i.e. feature coding that significantly impacts image classification in terms of both accuracy and speed. In proposed system, content based image retrieval (CBIR) system uses feature coding technique for image classification. As per paper [1], super vector coding (SVC) is the best coding method among all the methods of feature coding. In [23], using local visual descriptors a new framework i.e. SVC introduced for image classification. In this framework, a nonlinear feature transformation on descriptors performed, and then the results are combined to form an image-level representation, and lastly a classification model applied.

A. Mathematical Model

The system S is defined as:

$$S = \{I, Fd, F, Fv, Sv, O, I_4, IFv\}$$

The LBP operator on facial expression analysis and recognition is successfully reported in [22] and [23]. Xi Li *et al.* proposed a multiscale heat-kernel-based face representation as heat kernels are known to perform well in characterizing the topological structural information of face appearance. Furthermore, the LBP descriptor is incorporated into multiscale heat-kernel face representation for the purpose of capturing texture information of the face appearance [24]. Zhang *et al.* proposed local derivative patterns (LDPs) for face recognition, where they considered the LBP as nondirectional first-order local patterns collected from the first-order derivatives and extended the same approach for th order LDPs [25]. Lei *et al.* [26] proved that exploiting the image information jointly in image space, scale, and orientation domains can provide richer clues, which are not evident in any one individual domain. This process involves two phases. In the first phase, the face image is decomposed into different scale and orientation responses by convolving with multiscale and multiorientation Gabor filters. In the second phase, LBP analysis is used to describe the neighboring relationship not only in image space but also in different scale and orientation responses.

Zhao *et al.* proposed a local spatiotemporal descriptor using the LBP to represent and recognize spoken isolated phrases solely based on visual input [27]. Spatiotemporal LBPs extracted from mouth regions are used for describing isolated phrase sequences. Su *et al.* proposed the hybrid technique for graphic retrieval with the LBP and the Haar wavelet referred as structured local binary Haar pattern that encodes the polarity rather than the magnitude of the difference between accumulated gray values of adjacent rectangles [28]. The LBP has been also used for texture segmentation [29], background modeling and detection [30], shape localization [31], interest region description [32], and biomedical image retrieval [33]. The versions of the LBP and the LDP in the open literature cannot adequately deal with the range of appearance variations that commonly occur in unconstrained natural images due to illumination, pose, facial expression, aging, partial occlusions, etc. In order to address this problem, the local ternary pattern (LTP) [34] has been introduced for face recognition under different lighting conditions.

The LBP, the LDP, and the LTP extract the information based on the distribution of edges, which are coded using only two directions (positive direction or negative direction). Thus, it is evident that the performance of these methods can be improved by differentiating the edges in more than two directions. This observation has motivated us to propose the four direction code, referred to as local tetra patterns (LTrPs) for CBIR.

C. Main Contribution

In this paper, we propose a second-order LTrP that is calculated based on the direction of pixels using horizontal and vertical derivatives. Our method is different from the existing LDP in a manner that it makes use of 0 and 90 derivatives of LDPs for further calculating the directionality of each pixel. The performance resulting from the combination of theGT and the LTrP has been also analyzed. Finally, the generalized th-order LTrP

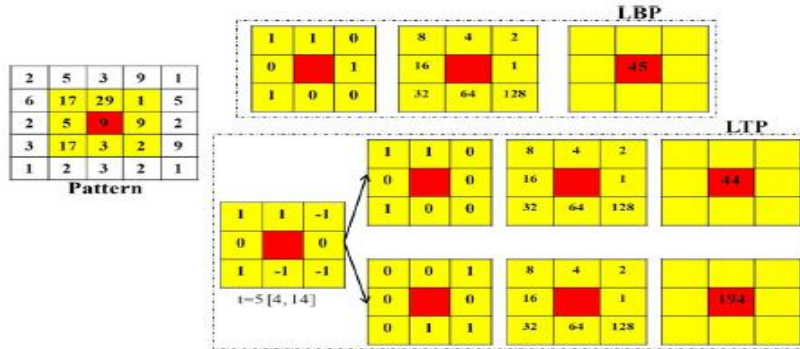


Fig. 1 Calculation of the LBP and LTP operators.

In the LTP, the obtained ternary pattern is further coded into upper and lower binary patterns. The upper pattern is obtained by retaining 1 and replacing 0 for 1 and 0. Lower pattern is coded by replacing 1 with 1 and 0 for 1 and 0. operator has been presented by using th-order derivatives The performance of our method is compared with the LBP, the LDP, and the LTP by conducting three experiments on different image database. Similar to LDP, in order to compare our method with the LBP, we consider the LBP as a nondirectional first-order local pattern called the *first-order* LTrP. The organization of this paper is as follows: In Section I, a brief review of the texture image retrieval and of related work is given. Section II presents a concise review of local patterns (the LBP, the LDP, the LTP, and the LTrP). Section III presents the concept of multiscale feature extraction, proposed system framework, and query matching. Experimental results and discussions are presented in Section IV, and finally, in Section V, we conclude with the summary of this paper and indicate possible future work.

II. LOCAL PATTERNS

A. LBPs

LBP operator was introduced by in [16] for texture classification. Given a center pixel in the image, the LBP value is computed by comparing its gray value with its neighbors, as shown in Fig. 1, based on

$$LBP_{P,R} = \sum_{p=1}^P 2^{(p-1)} \times f_1(g_p - g_c) \quad (1)$$

$$f_1(x) = \begin{cases} 1, & x \geq 0 \\ 0, & \text{else} \end{cases} \quad (2)$$

Where g_c is the gray value of the center pixel, g_p is the gray value of its neighbors, P is the number of neighbors, and R is the radius of the neighborhood.

B. LTPs

Tan and Triggs [34] extended the LBP to a three-valued code called the LTP, g_c in which gray values in the zone of width $+t$ around are quantized to zero, those above $(g_c + t)$ are quantized

to + 1, and those (g_c-t)below are quantized to -1, i.e., indicator f₁(x) is replaced with three-valued function (3) and the binary LBP code is replaced by a ternary LTP code, as shown in Fig. 1, i.e.,

$$\hat{f}_1(x, g_c, t) = \begin{cases} +1, & x \geq g_c + t \\ 0, & |x - g_c| < t \\ -1, & x \leq g_c - t \end{cases} \Big|_{x=g_p}$$

More details about LTP can be found in [34].

C. LDPs

]. Zhang *et al.* proposed the LDPs for face recognition [25]. They considered the LBP as the nondirectional first-order local pattern operator and extended it to higher orders (th-order) called the LDP. The LDP contains more detailed discriminative features as compared with the LBP.

To calculate the th-order LDP, the (n-1) th-order derivatives are calculated along 0⁰, 45⁰, 90⁰, and 135⁰ directions, denoted as . Finally, th-order LDP is calculated as

$$LDP_{\alpha}^n(g_c) = \sum_{p=1}^r 2^{(p-1)} \times f_2 \left(I_{\alpha}^{(n-1)}(g_c), I_{\alpha}^{(n-1)}(g_p) \right) \Big|_{P=8} \tag{4}$$

$$f_2(x, y) = \begin{cases} 1, & \text{if } x.y \leq 0 \\ 0, & \text{else.} \end{cases} \tag{5}$$

The detailed discussion and the sample example for the LDP calculation are available in [25].

D. LTRPs

The idea of local patterns (the LBP, the LDP, and the LTP) proposed in [16], [25], and [34] has been adopted to define LTRPs. The LTrP describes the spatial structure of the local texture using the direction of the center gray pixel . Given image , I the first-order derivatives along 0⁰ and 90⁰ directions are denoted as I_{g(g_p)}¹|_{0=0⁰..,90⁰ Let g_c denote the center pixel in ,g_h and g_v let and denote the horizontal and vertical neighborhoods of g_c , respectively. Then, the first-order derivatives at the center pixel g_c can be written as}

$$I_{0^0}^1(g_c) = I(g_h) - I(g_c) \tag{6}$$

$$I_{90^0}^1(g_c) = I(g_v) - I(g_c) \tag{7}$$

and the direction of the center pixel can be calculated as

$$I_{Dir}^1(g_c) = \begin{cases} 1, & I_{0^0}^1(g_c) \geq 0 \text{ and } I_{90^0}^1(g_c) \geq 0 \\ 2, & I_{0^0}^1(g_c) < 0 \text{ and } I_{90^0}^1(g_c) \geq 0 \\ 3, & I_{0^0}^1(g_c) < 0 \text{ and } I_{90^0}^1(g_c) < 0 \\ 4, & I_{0^0}^1(g_c) \geq 0 \text{ and } I_{90^0}^1(g_c) < 0. \end{cases} \tag{8}$$

From (8), it is evident that the possible direction for each center pixel can be either 1, 2, 3, or 4, and eventually, the image is converted into four values, i.e., directions.

$$LTrP^2(g_c) = \{ f_3 (I_{Dir}^1(g_c), I_{Dir}^1(g_1)), f_3 (I_{Dir}^1(g_c), I_{Dir}^1(g_2)), \dots, f_3 (I_{Dir}^1(g_c), I_{Dir}^1(g_P)) \} \Big|_{P=8} \tag{9}$$

$$f_3 (I_{Dir}^1(g_c), I_{Dir}^1(g_p)) = \begin{cases} 0, & I_{Dir}^1(g_c) = I_{Dir}^1(g_p) \\ I_{Dir}^1(g_p), & \text{else.} \end{cases} \tag{10}$$

The second-order LTrP² (q_c)defined as

From (9) and (10), we get 8-bit tetra pattern for each center pixel. Then, we separate all patterns into four parts based on the direction of center pixel. Finally, the tetra patterns for each part (direction) are converted to three binary patterns. Let the direction of center pixel obtained using (8) be “1”; then, can be defined by segregating it into three binary patterns as follows:

$$= \sum_{p=1}^P 2^{(p-1)} \times f_4 (LTrP^2(g_c)) \Big|_{\text{Direction}=2,3,4} \quad (11)$$

$$f_4 (LTrP^2(g_c)) \Big|_{\text{Direction}=\phi} = \begin{cases} 1, & \text{if } LTrP^2(g_c) = \phi \\ 0, & \text{else} \end{cases} \quad (12)$$

where .

Similarly, the other three tetra patterns for remaining three directions (parts) of center pixels are converted to binary patterns. Thus, we get 12 (4 * 3) binary patterns.

Guo *et al.* [20] used the magnitude component of the local difference operator to propose the magnitude LBP, along with the sign LBP for texture classification. They proved that, although the sign component extracts more useful information as compared with the magnitude component, exploiting the combination of sign and magnitude components can provide better clues, which are not evident in any one individual component. This concept has motivated us to propose the 13th binary pattern (LP) by using the magnitudes of horizontal and vertical first-order derivatives using

$$M_{I^1(g_p)} = \sqrt{(I_{0^\circ}^1(g_p))^2 + (I_{90^\circ}^1(g_p))^2} \quad (13)$$

$$LP = \sum_{p=1}^P 2^{(p-1)} \times f_1 (M_{I^1(g_p)} - M_{I^1(g_c)}) \Big|_{P=8} \quad (14)$$

For the local pattern with neighborhoods, 2^P combinations of LBPs are possible, resulting in the feature vector length of 2^P . The computational cost of this feature vector is very high. In order to reduce the computational cost, we consider the uniform patterns [18]. The uniform pattern refers to the uniform appearance pattern that has limited discontinuities in the circular binary representation. In this paper, those patterns that have less than or equal to two discontinuities in the circular binary representation are referred to as the uniform patterns, and the remaining patterns are referred to as nonuniform. $P(P-1)+2$ Thus, the distinct uniform patterns for a given query image would be . The possible uniform patterns $P=8$ for can be seen in [18]. After identifying the local pattern PTN (the LBP, the LTP, the LDP, or the 13-binary-pattern form LTrP), the whole image is represented by building a histogram using

$$H_S(l) = \frac{1}{N_1 \times N_2} \sum_{j=1}^{N_1} \sum_{k=1}^{N_2} f_5 (PTN(j, k), l); \quad (15)$$

$$l \in [0, P(P-1) + 2]$$

$$f_5(x, y) = \begin{cases} 1, & \text{if } x = y \\ 0, & \text{else} \end{cases} \quad (16)$$

Where $(N_1 * N_2)$ represents the size of the input image.

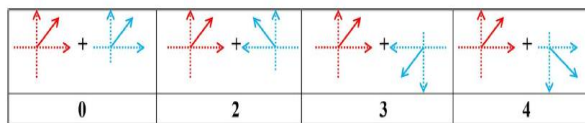


Fig. 2. Calculation of tetra pattern bits for the center-pixel direction “1” using the direction of neighbors. Direction of (red) the center pixel and (cyan) that its neighborhood pixels.

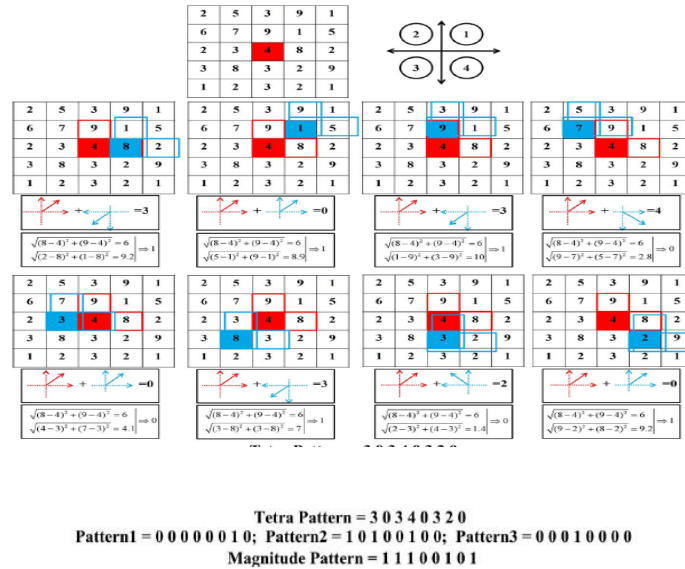


Fig. 3. Example to obtain the tetra and magnitude patterns.

For generating a tetra pattern, the bit is coded with the direction of neighbor when the direction of the center pixel and its neighbor are different, otherwise “0.” For the magnitude pattern, the bit is coded with “1” when the magnitude of the center pixel is less than the magnitude of its neighbor, otherwise “0.”

Fig. 2 illustrates the possible local pattern transitions resulting in an LTrP for direction “1” of the center pixel. The LTrP is coded to “0” when it is equal to the direction of center pixel, otherwise coded in the direction of neighborhood pixel. Using the same analogy, LTrPs are calculated for center pixels having directions 2, 3, and 4. An example of the second-order LTrP computation resulting in direction “1” for a center pixel marked with red has been illustrated in Fig. 3. When we apply first-order derivative in horizontal and vertical directions to the neighborhood pixel “8,” we obtain direction “3” and magnitude “9.2.” Since the direction of the center pixel and the direction obtained from the neighborhood pixel are not same, we assign value “3” to the corresponding bit of the LTrP. It can be seen that the magnitude of the center pixel is “6,” which is less than the magnitude of neighborhood pixel. Hence, we assign value “1” to the corresponding bit of the magnitude pattern. Similarly, the remaining bits of the LTrP and the magnitude pattern for the other seven neighbors are computed resulting in the tetra pattern “3 0 3 4 0 3 2 0” and the magnitude binary pattern “1 1 1 0 0 1 0 1.” After coding the tetra pattern, we separate it into three binary patterns as follows. Referring to the generated LTrP, the first pattern is obtained by keeping “1” where the tetra pattern value is “2” and “0” for other values, i.e., “0 0 0 0 0 1 0.” Similarly, the other two binary patterns “1 0 1 0 0 1 0 0” and “0 0 0 1 0 0 0 0” are computed for tetra pattern values “3” and “4,” respectively. In the same way, tetra patterns for center pixels having directions 2, 3, and 4 are computed. Thus, with four tetra patterns, 12 binary patterns are obtained. The 13th binary pattern is obtained from the magnitude of the first-order derivatives

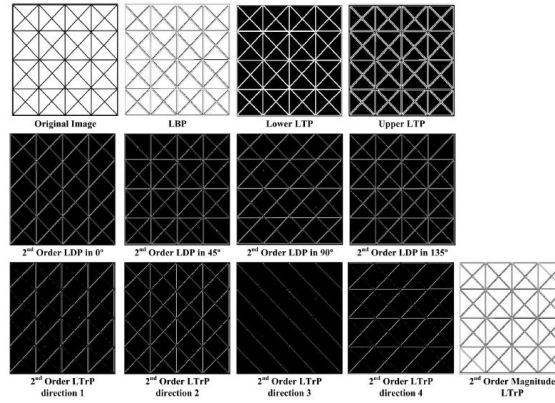


Fig. 4 Each pixel of the original image is considered as the center pixel, and it is coded by using the LBP, LTP, LDP, and LTrP descriptors with the help of neighbors.

The possible values of various descriptors are in between 0 to 255, which are further used for dimension reduction by uniform patterns. The LTrP extracts additional directional information, as compared with other patterns.

E. N th-Order LTrPs

To calculate the third-order tetra pattern, initially, the second order derivatives along horizontal and vertical directions, denoted as $I^2_0(g_p)|_{0=0^0, 90^0}$ are computed. Using these derivatives, the third-order tetra pattern is $LTrP^3(g_c)$ defined as

$$LTrP^3(g_c) = \{ f_3(I^2_{Dir.}(g_c), I^2_{Dir.}(g_1)), f_3(I^2_{Dir.}(g_c), I^2_{Dir.}(g_2)), \dots, f_3(I^2_{Dir.}(g_c), I^2_{Dir.}(g_P)) \} |_{P=8} \quad (17)$$

The generalized formulation for the th-order LTrP can be defined by using(n-1) th-order derivatives in horizontal and vertical directions $I^{n-1}_0(g_p)|_{0=0^0, 90^0}$ as

$$LTrP^n(g_c) = \{ f_3(I^{n-1}_{Dir.}(g_c), I^{n-1}_{Dir.}(g_1)), f_3(I^{n-1}_{Dir.}(g_c), I^{n-1}_{Dir.}(g_2)), \dots, f_3(I^{n-1}_{Dir.}(g_c), I^{n-1}_{Dir.}(g_P)) \} |_{P=8} \quad (18)$$

The higher order LTrPs have the capability to extract more detailed information as compared with lower order LTrPs. However, it has been observed that the second-order LTrP provides better performance as compared with higher order LTrPs (refer to Section IV). This is primarily because higher order LTrPs are more sensitive to noise Fig. 4 illustrates the results obtained by applying the LBP, LTP, LDP, and LTrP operators on a reference image. The reference image has been chosen since it provides the results that are visibly comprehensible to differentiate the effectiveness of these approaches. It can be observed that the second-order LTrP operator is able to extract detailed directional information, as compared with second-order LDP, LBP, and LTP operators.

F. Advantages of the LTrP Over Other Patterns

The advantages of the LTrP over the LBP, the LDP, and the LTP can be justified with the help of three points.

- 1) The LBP, the LDP, and the LTP are able to encode image with only two (either “0” or “1”), two (either “0” or “1”), and three (“0,” “1,” or “1”) distinct values, respectively. However, the LTrP is able to encode images with four distinct values as it is able to extract more detailed information (refer to Fig. 4).

2) The LBP and the LTP encode the relationship between the gray value of the center pixel and its neighbors, whereas the LTrP encodes the relationship between the center pixel and its neighbors based on directions that are calculated with the help of (n-1) th-order derivatives.

3) The LDP encodes the relationship between the (n-1) th-order derivatives of the center pixel and its neighbors in 0° , 45° , 90° , and 135° directions separately, whereas the LTrP encodes the relationship based on the direction of the center pixel and its neighbors, which are calculated by combining (n-1) th-order derivatives of the 0° and 90° directions.

III. MULTISCALE FEATURE EXTRACTION

The GT can provide good directional information for texture analysis. Furthermore, the LDP, LTP, and LBP methods also make use of the GT to analyze the effectiveness of their methods for applications in pattern recognition. Thus, in order to compare our results with the aforementioned methods, we have presented the analysis of our method (the LTrP) with the GT.

A. GT

Subrahmanyam *et al.* [35] have given the spatial implementation of the GT. A 2-D Gabor function is a Gaussian modulated by a complex sinusoid. It can be specified by the frequency of sinusoid and the standard deviations and of the Gaussian envelope as follows:

$$G_{mn}(x, y) = \sum_s \sum_t I((x - s, y - t) \psi_{mn}^*(s, t)). \quad (20)$$

The response of the Gabor filter is the convolution of the Gabor window with image and is given by

$$\psi(x, y) = \frac{1}{2\pi\sigma_x\sigma_y} e^{[-(1/2)(x^2/\sigma_x^2 + y^2/\sigma_y^2) + 2\pi j\omega x]}.$$

B. Proposed System Framework

Fig. 5 illustrates the flowchart of the proposed image retrieval system and algorithm as given below.

Algorithm:

Input: Query image; Output: Retrieval result

1. Load the image, and convert it into grayscale.
2. Apply the first-order derivatives in horizontal and vertical axis.
3. Calculate the direction for every pixel.
4. Divide the patterns into four parts based on the direction of the center pixel.
5. Calculate the tetra patterns, and separate them into three binary patterns.
6. Calculate the histograms of binary patterns.
7. Calculate the magnitudes of center pixels using (13).
8. Construct the binary patterns, and calculate their histogram.
9. Combine the histograms calculated from steps 6 and 8.
10. Construct the feature vector.
11. Compare the query image with the images in the database using (24).
12. Retrieve the images based on the best matches.

This algorithm is also applied on Gabor wavelet subbands (with three scales and two directions) for GLTrP.

IV. CONCLUSION

In this experiment, database DB3 is used, which consists of 40 different textures collected from the MIT VisTex database [39]. The size of each texture is 512 * 512. Each 512 * 512 image is divided into sixteen 128 * 128 non-overlapping sub-images, thus

creating a database of 640 (40 16) images. The performance of the proposed method is measured in terms of ARR computed using (30). Database DB3 has been used to compare the performance of the LTrP with other existing methods (the LTP, the LDP, and the LBP) with and without GT. From Table I, it is evident that the LTrP/GLTrP outperforms other existing methods. Fig. 12 shows the graphs illustrating the retrieval performance of the LTrP/ GLTrP and other existing methods as a function of the number of top matches. Fig. 13 shows the comparison between different orders of LTrPs and LDPs with and without GT in terms of ARR. From Table I and Figs. 12 and 13, it is evident that the LTrP/ GLTrP yields better performance as compared with the other existing methods.

REFERENCES

- [1] Y. Rui and T. S. Huang, "Image retrieval: Current techniques, promising directions and open issues," *J. Visual Commun. Image Represent.*, vol. 10, no. 1, pp. 39–62, Mar. 1999.
- [2] A. W. M. Smeulders, M. Worring, S. Santini, A. Gupta, and R. Jain, "Content-based image retrieval at the end of the early years," *IEEE Trans. Pattern Anal. Mach. Intell.*, vol. 22, no. 12, pp. 1349–1380, Dec. 2000.
- [3] M. Kokare, B. N. Chatterji, and P. K. Biswas, "A survey on current content based image retrieval methods," *IETE J. Res.*, vol. 48, no. 3&4, pp. 261–271, 2002.
- [4] Y. Liu, D. Zhang, G. Lu, and W.-Y. Ma, "A survey of content-based image retrieval with high-level semantics," *Pattern Recogn.*, vol. 40, no. 1, pp. 262–282, Jan. 2007.
- [5] H. A. Moghaddam, T. T. Khajoie, and A. H. Rouhi, "A new algorithm for image indexing and retrieval using wavelet correlogram," in *Proc. ICIP*, 2003, pp. III-497–III-500.
- [6] H. A. Moghaddam and M. Saadatmand Tarzjan, "Gabor wavelet correlogram algorithm for image indexing and retrieval," in *Proc. ICPR*, 2006, pp. 925–928.
- [7] M. Saadatmand Tarzjan and H. A. Moghaddam, "A novel evolutionary approach for optimizing content based image retrieval," *IEEE Trans. Syst., Man, Cybern. B, Cybern.*, vol. 37, no. 1, pp. 139–153, Feb. 2007.
- [8] A. Ahmadian and A. Mostafa, "An efficient texture classification algorithm using gabor wavelet," in *Proc. EMBS*, 2003, pp. 930–933.
- [9] M. N. Do and M. Vetterli, "Wavelet-based texture retrieval using generalized Gaussian density and Kullback–Leibler distance," *IEEE Trans. Image Process.*, vol. 11, no. 2, pp. 146–158, Feb. 2002.
- [10] M. Unser, "Texture classification by wavelet packet signatures," *IEEE Trans. Pattern Anal. Mach. Intell.*, vol. 15, no. 11, pp. 1186–1191, Nov. 1993.
- [11] B. S. Manjunath and W. Y. Ma, "Texture features for browsing and retrieval of image data," *IEEE Trans. Pattern Anal. Mach. Intell.*, vol. 18, no. 8, pp. 837–842, Aug. 1996.
- [12] M. Kokare, P. K. Biswas, and B. N. Chatterji, "Texture image retrieval using rotated wavelet filters," *Pattern Recogn. Lett.*, vol. 28, no. 10, pp. 1240–1249, Jul. 2007.
- [13] M. Kokare, P. K. Biswas, and B. N. Chatterji, "Texture image retrieval using new rotated complex wavelet filters," *IEEE Trans. Syst., Man, Cybern. B, Cybern.*, vol. 35, no. 6, pp. 1168–1178, Dec. 2005.
- [14] M. Kokare, P. K. Biswas, and B. N. Chatterji, "Rotation-invariant texture image retrieval using rotated complex wavelet filters," *IEEE Trans. Syst., Man, Cybern. B, Cybern.*, vol. 36, no. 6, pp. 1273–1282, Dec. 2006.
- [15] T. Ojala, M. Pietikainen, and D. Harwood, "A comparative study of texture measures with classification based on feature distributions," *Pattern Recogn.*, vol. 29, no. 1, pp. 51–59, Jan. 1996.
- [16] T. Ojala, M. Pietikainen, and T. Maenpää, "Multiresolution gray-scale and rotation invariant texture classification with local binary patterns," *IEEE Trans. Pattern Anal. Mach. Intell.*, vol. 24, no. 7, pp. 971–987, Jul. 2002.
- [17] M. Pietikainen, T. Ojala, T. Scruggs, K. W. Bowyer, C. Jin, K. Hoffman, J. Marques, M. Jacsik, and W. Worek, "Rotational invariant texture classification using feature distributions," *Pattern Recogn.*, vol. 33, no. 1, pp. 43–52, Jan. 2000.